The Effect Of The Free Surface On Penetration Depth Limited X-ray Stress Measurements

Thomas Gnaupel-Herold

Center for Neutron Research, National Institute of Standards and Technology

100 Bureau Dr. M/S 6102, Gaithersburg, MD, 20899-6102, USA

ABSTRACT

The elastic behaviour of grains bordering a free surface is analysed through the self-consistent grain-matrix interaction model. The approach proposed here assumes in-plane stresses and free Poisson expansion or contraction in the normal direction; in-plane grain- matrix interaction remains active for surface grains. Grains at greater depths interact with the matrix in the usual way, thus producing two distinct results for the surface and for the bulk. The effective diffraction response for surface limited X-rays is the attenuation-length weighted average of surface grains and bulk grains. The existing self-consistent models can be easily adapted to the surface effect to include preferred orientation and non-spherical grains. An important consequence of the surface effect is that materials consisting of elastically anisotropic grains exhibit nonlinear lattice strain vs. $\sin^2\psi$ distributions even without texture. In practice, the effect can be minimized by large tilt angle ranges, penetration depths larger than the grain size, or under-sampling lattice strains at low tilt angles.

Keywords: X-ray elastic constants, surface effect

INTRODUCTION

The elastic behaviour of ellipsoidal inclusions in the presence of a free surface has been studied for decades. Mindlin [1] calculated stresses for spherical inclusions arising from different thermal expansion coefficients near a free surface. It was shown that the proximity of the free surface induces non-uniform stresses and strains inside the inclusion. Seo and Mura [2], [3] expanded further by considering ellipsoidal grains, and by calculating the effect of the ellipsoid axis parameters and the distance from the surface. The distance-dependent interior strains represent a crucial difference to Eshelby's findings [4] of uniform interior strains in ellipsoidal grains embedded in an infinite elastic space. Eshelby's result of constant interior strains is the underpinning of self-consistent calculations of elastic constants because it avoids difficult pointwise calculations of strains and the subsequent determinations of the volume averages for each grain. Welzel [5] modelled the surface effect for thin films using a linear combination of model results from Vook-Witt [6], Reuss [7], and Voigt [8]. The method allowed for the consideration of effects of preferred orientation. The pointwise computation of strains based on prescribed states of strain and stress was done again recently by Mareau [9] who calculated the isotropic X-ray elastic constants (XEC) $s_1(hkl)$ and $\frac{1}{2}s_2(hkl)$ in the bulk limit (the familiar case) and in the surface limit. He introduced the ratio of grain size to penetration depth as a determinant for the magnitude of the surface effect. The terms X-ray elastic constants (XEC) and diffraction elastic constants (DEC) used in the literature refer to the same property; however, the effect discussed here is accessible only to X-ray diffraction with suitably low penetration depths, and the term XEC will be used from here on forward.

In this work it will be shown that results very similar to Mareau's can be obtained for the self-consistent models, also known as Kröner models [10], [11], from the condition that surface grains can freely contract or expand along the surface normal while grain-matrix interaction remains in place for in-plane directions. This approach is computationally simple, and existing self-consistent codes can be easily modified. The generalization to preferred grain orientation and non-spherical grain shapes can be done without difficulties.

The Effect Of The Free Surface On Penetration Depth Limited X-ray Stress Measurements" Gnaupel-Herold, T., in 2024 SEM Annual Conference, Downloadable Submissions, (Society for Experimental Mechanics, Vancouver, WA, 2024), pp. 1–9

MODELLING

The self-consistent approach based on the Eshelby-Kröner model [12] has been widely used for calculating both aggregate (bulk) elastic constants ([13], [14]) and diffraction elastic constants [10], [11], [15]. In particular, the built-in concept of grain-matrix interaction addresses the shortcomings of interaction-free models in which the elastic properties of material surrounding a grain are disregarded. From basic considerations it can be expected that for surface grains a different degree of grain-matrix interaction can be expected compared to grains in the bulk because in-plane stresses induce Poisson strains that are unimpeded along the direction of the surface normal. The mediating effect of neighbouring grains within the surface plane is the same as for bulk grains, therefore inducing elastic anisotropy in the matrix directly at the surface but not for grains below the surface layer. Laboratory source X-ray strain measurements commonly measure lattice strain over different tilt angles ψ with respect to the surface normal (Figure 1) which, in the absence of both texture and surface effect, result in linear distributions of ε vs $\sin^2\psi$. With surface effect it can be expected that the lattice strains of surface grains, depending on the tilt angle, reflect different portions of the local matrix anisotropy, therefore inducing a degree of non-linearity into ε vs $\sin^2\psi$ distributions. The following, more detailed, considerations are based on the coordinate frames in Figure 1.

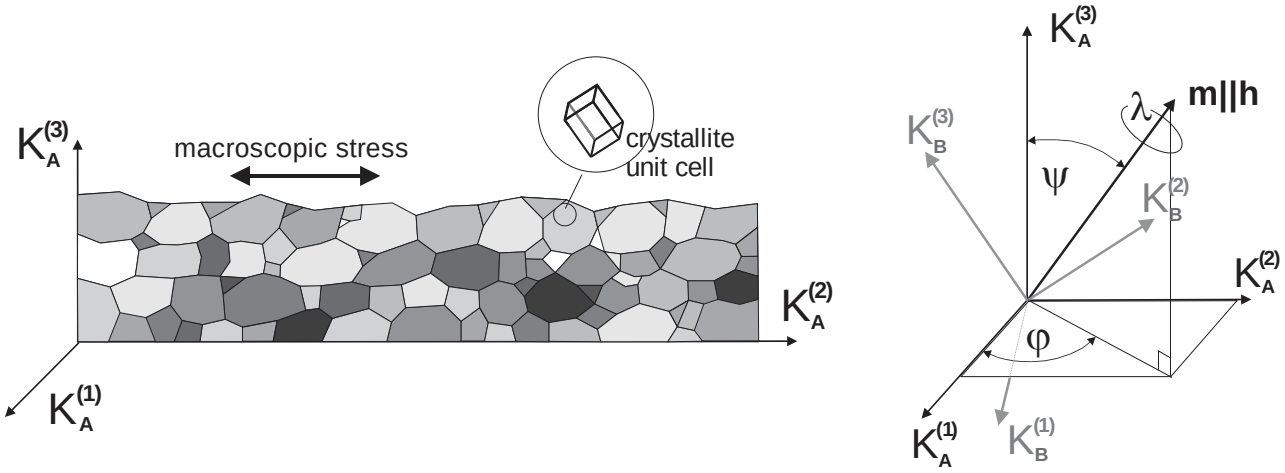

Figure 1 : Coordinate systems of the sample (K_A) and of the crystallite (K_B) for the surface grains. The direction of the scattering vector **m**||**h** is given by the spherical polar angles (φ,ψ). The lattice vector **h** is the normal of the lattice plane with Miller indices (hkl) used in the diffraction measurement.

The condition of unrestricted normal strains for surface grains can be written as

$$\bar{\varepsilon}_{33} = \varepsilon_{33}(g) \tag{1}$$

Here, $\bar{\varepsilon}_{33}$ is the macroscopic strain of the matrix perpendicular to the surface and $\varepsilon_{33}(g)$ is the strain of a crystallite with orientation g, g being the orientation matrix. The calculation of g from (hkl), unit cell data, and the direction (φ,ψ) is described in detail in [16]. Equation (1) states that for surface grains the strain $\bar{\varepsilon}_{33}$ of the matrix is made equal to the strain in the grain with orientation g. The condition (1) is imposed for each grain at the surface with an orientation that fulfils **m**||**h**. In other words, the matrix Poisson strain is locally adapted to the Poisson strain for each grain specifically. One has

$$\varepsilon_{33}(g) = s_{3311}(g)\bar{\sigma}_{11} + s_{3322}(g)\bar{\sigma}_{22} = S_{3311}\bar{\sigma}_{11} + S_{3322}\bar{\sigma}_{22} \tag{2}$$

The $s_{33kk}(g)$ are components of the rotated single crystal stiffnesses. The S_{ijkl} are the matrix elastic constants. It follows for each grain that

$$S_{3311} = s_{3311}(g);\ \ S_{3322} = s_{3322}(g) \tag{3}$$

The condition (3) ensures unrestricted Poisson strains for grains with orientation g.

The relationship between lattice strain and applied stress can be expressed through a tensor where the direction **m**||**h** of measured lattice strain corresponds to the z-direction of an intermediate frame K as shown in [16]. It is written as

$$\varepsilon(hkl,\varphi,\psi) = \overline{a_{33kl}}(hkl,\varphi,\psi)\bar{\sigma}_{kl} \tag{4}$$

The $\overline{a_{33kl}}(hkl,\varphi,\psi)$ are generalized compliances which are expressed as the stress factors $F_{kl}(hkl,\varphi,\psi)$ with

$$F_{kl} = \overline{a_{33kl}}(hkl,\varphi,\psi) \tag{5}$$

Stress factors relate lattice strains to macroscopic stresses. The upper/lower bound self-consistent models for DEC/XEC stress factors contain a measure of grain-matrix interaction that can be used to quantify the surface effect. Here, the formulas developed by Behnken [10] are used:

$$a_{ijkl}(g) = S_{ijkl} + u_{ijmn}(g)S_{mnkl} \tag{6}$$

$$u_{ijkl}(g) = u_{ijkl}(g) = -v^{-1}_{ijmn}(g)[c_{mnkl}(g) - C_{mnkl}] \tag{7}$$

$$v_{ijkl}(g) = c_{ijkl}(g) - C_{ijkl} + C_{ijmn}w_{mnkl}$$

The S_{ijkl} and C_{ijkl} are the compliances and stiffnesses of the matrix; the $c_{mnkl}(g)$ are the orientation dependent stiffnesses of the grain and w_{mnkl} is the inverse of the Eshelby tensor [4] and $u_{ijkl}(g)$ and $v_{ijkl}(g)$ are intermediate expressions. The stress factors from equation (5) characterize the average strain response of grains contributing to the reflection (hkl), and the orientation average over all rotations about **m**||**h** must be calculated. In the case of texture the orientation weight $f(g)$ (multiples of random density) must be included, leading to the expression

$$F_{kl}(hkl,\varphi,\psi) = \overline{a_{33kl}} = \frac{m_i m_j \int_0^{2\pi} a_{ijkl}(g) f(g) d\lambda}{\int_0^{2\pi} f(g) d\lambda}, \qquad i,j,k,l = 1..3 \tag{8}$$

The m_i are the components of the vector **m** in spherical polar coordinates with **m**=($\cos\varphi \sin\psi$, $\sin\varphi \sin\psi$, $\cos\psi$). Detailed recipes for the calculation the orientation matrix g as a function of (hkl), crystal symmetry, and the angles λ, φ, and ψ are given in [11].

The XEC surface values are obtained by replacing S_{3311} and S_{3322} with the orientation dependent values for each grain orientation according to equation (3). For consistency, the thus obtained matrix compliance tensor must be inverted to obtain the matrix stiffnesses C_{ijkl} which are subsequently used to calculate the inverse Eshelby tensor. All calculations must be done for each grain orientation in equation (8). Also, appropriate elastic symmetry of the matrix at the surface must be applied in calculations of the Eshelby tensor which is generally transversal isotropic or orthorhombic. In contrast, the bulk XEC are obtained the usual way, that is, without applying equation (3).

X-ray attenuation determines the relative contribution of the surface grain XEC vs. XEC of subsurface or bulk grains. Assuming that both surface XEC and bulk XEC are constant (independent on depth) the effective XEC can be calculated using the weights w_s (surface) and w_b (bulk). The latter are obtained from

$$w_s = \frac{\int_0^{g_z} z\, e^{-z/\tau} dz}{\int_0^{\infty} e^{-z/\tau} dz} = 1 - \left(\frac{g_z}{\tau} + 1\right) e^{-g_z/\tau} \tag{9}$$

$$w_b = \frac{\int_{g_z}^{\infty} z\, e^{-z/\tau} dz}{\int_0^{\infty} e^{-z/\tau} dz} = \left(\frac{g_z}{\tau} + 1\right) e^{-g_z/\tau} = 1 - w_{surf} \tag{10}$$

Here, z is the coordinate in the direction normal to the surface, g_z is the z-dimension of the grains, and τ is the attenuation length calculated for the most common diffraction geometry (ψ-mode, tilt axis parallel to the scattering plane) [17]

$$\tau_\psi = \frac{\sin\theta\cos\psi}{2\mu} \tag{11}$$

ψ was defined in Figure 1, θ is the Bragg angle; μ is the attenuation coefficient specific for the X-ray wavelength used and the material being investigated. The final expression for the effective, attenuation-weighted XEC is

$$F_{kl}^{eff}(hkl,\varphi,\psi) = w_s F_{kl}^{s}(hkl,\varphi,\psi) + w_{bulk} F_{kl}^{b}(hkl,\varphi,\psi) \tag{12}$$

The distinction between surface XEC and bulk XEC is a binary one, and the surface effect is considered uniform through the thickness of the surface grains, therefore overestimating the effect. This assumption was made to avoid the otherwise necessary pointwise calculations of strain in single grains and subsequent volume averages as done in [9]. Also, such calculations do not necessarily produce more accurate results. All grains below the surface grains are treated as bulk for the same reason which underestimates the surface effect in the deeper layers; however, the calculation of the effective XEC in (12) produces a single XEC value. For isotropic sample symmetry, the often-used XEC $s_1(hkl)$ and $\frac{1}{2}s_2(hkl)$ can be obtained from the F_{kl} using, for example (more such relations exist),

$$s_1(hkl) = F_{11}(hkl,0,0) = F_{22}(hkl,0,0) = F_{33}(hkl,0,90°) = F_{22}(hkl,0,90°) \tag{13}$$

$$\frac{1}{2}s_2(hkl) = F_{33}(hkl,0,0) - F_{11}(hkl,0,0) = F_{11}(hkl,0,90°) - F_{33}(hkl,0,90°) \tag{14}$$

Equations (13) and (14) will yield different results for the surface compared to the bulk. In a strict sense, $s_1(hkl)$ and $\frac{1}{2}s_2(hkl)$ should not be used for surface XEC because the matrix at the surface is principally anisotropic, thus leading to non-linear d($\sin^2\psi$) distributions. In practice, the effect is often small as shown in the following.

RESULTS

For clarity the following discussion will be limited to cubic materials because findings on elastic anisotropy are more easily expressed; however, the methods outlined above apply to all crystal symmetries and sample symmetries. A comparison of results obtained using the model developed in this work with results obtained by Mareau [9] is shown in Figure 2. XEC were calculated using orthorhombic sample symmetry and spherical grains. The sample symmetry is contained in the symmetry of the stiffness and compliance tensor, and it only affects calculations of surface XEC.

The agreement with Mareau's results is good to excellent, thus demonstrating that the surface effect can be effectively quantified in a more generally usable way. The single crystal constants were taken from [18] and [19]. The differences between surface XEC and bulk values are shown in Figure 2. In relative terms, the differences are largest for the elastically softest crystal direction ([100] for both iron and aluminium). Note that XEC have the dimension of compliances; smaller positive values are elastically harder. For aluminium, being quite isotropic, the surface effect is very small with ≈ 2 % ($\frac{1}{2}s_2(hkl)$) to 5 % ($s_1(hkl)$) relative difference bulk-surface for the (100). Differences for all other (hkl) are even smaller. For the more anisotropic iron the largest relative differences for the (100) grow to ≈ 10 % ($\frac{1}{2}s_2(hkl)$) to 25 % ($s_1(hkl)$).

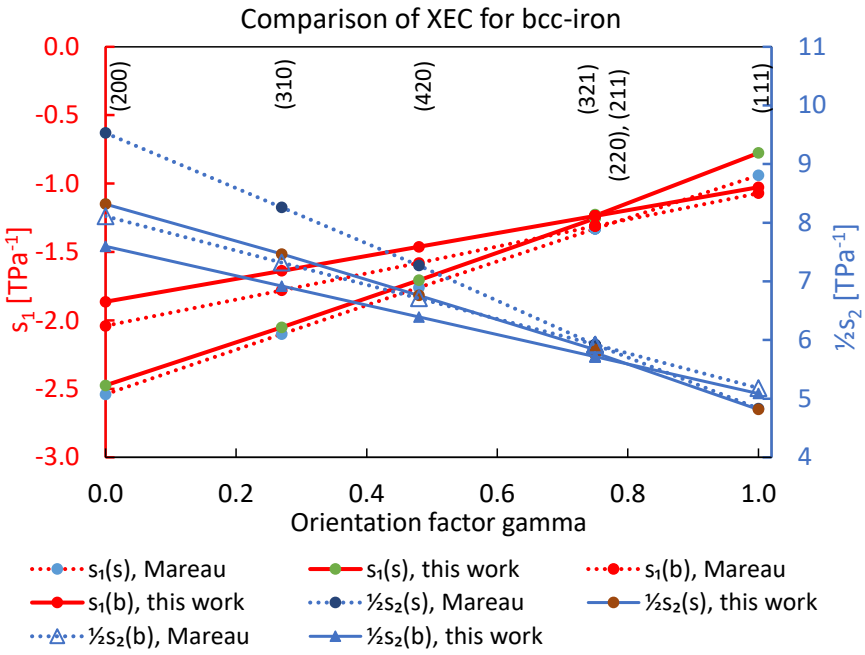

a)

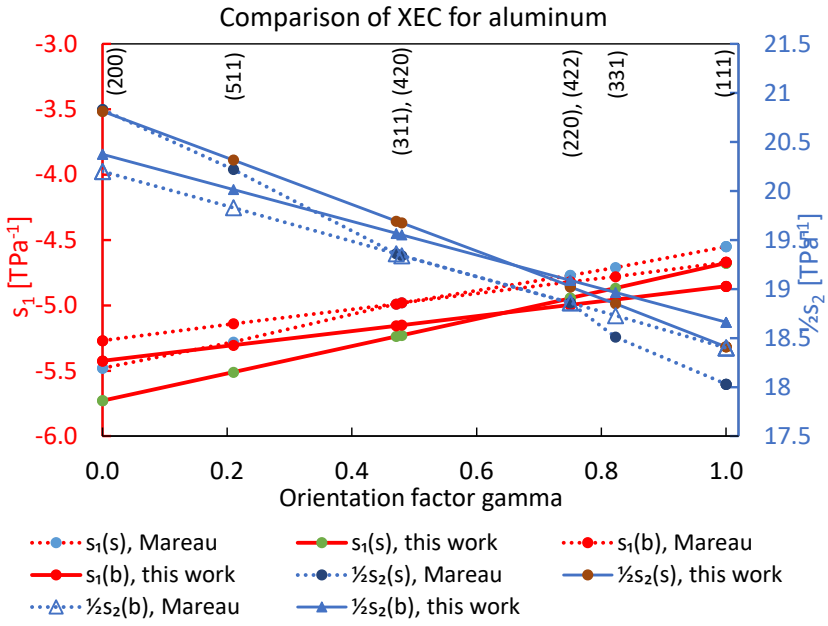

b)

Figure 2 Comparison of Mareau's [9] results and Kröner model results for iron (a) and aluminium (b). The $s_1(hkl)$ are shown in red with the vertical axis on the left of each plot. The $\frac{1}{2}s_2(hkl)$ are shown in blue with the vertical axis on the right side of each graph. The terms '(s)' and '(b)'refer to the surface and the bulk, respectively. The X-axis is the orientation factor $3\Gamma = \left(h^2k^2 + h^2l^2 + k^2l^2\right)\left(h^2 + k^2 + l^2\right)^{-2}$.

In practice, only soft X-rays from laboratory X-ray tubes with wavelengths >0.1 nm make the surface effect accessible. Lattice strain measurements usually involve different tilt angles ψ which changes both the penetration depth and the portions sampled of in-plane strain and normal strains where only the latter is susceptible to the surface effect. With increasing tilt angle the surface effect becomes smaller, and the XEC converge to the bulk values even at zero penetration depth as shown

in Figure 3 where orientation dependent stress factors are shown. Note that due to equation (4) stress factors show the same qualitative dependence on the tilt angle as lattice strains. The (211) reflection has almost no surface effect (Figure 3, right) because the orientation factor 3Γ(211)=0.75 is equal to the orientation average of an untextured cubic polycrystal; both grain-matrix interaction and the surface effect are smallest for this orientation as demonstrated in Figure 2 where surface XEC and bulk XEC intersect at 3Γ=0.75. The same applies to (321) and (220) oriented grains.

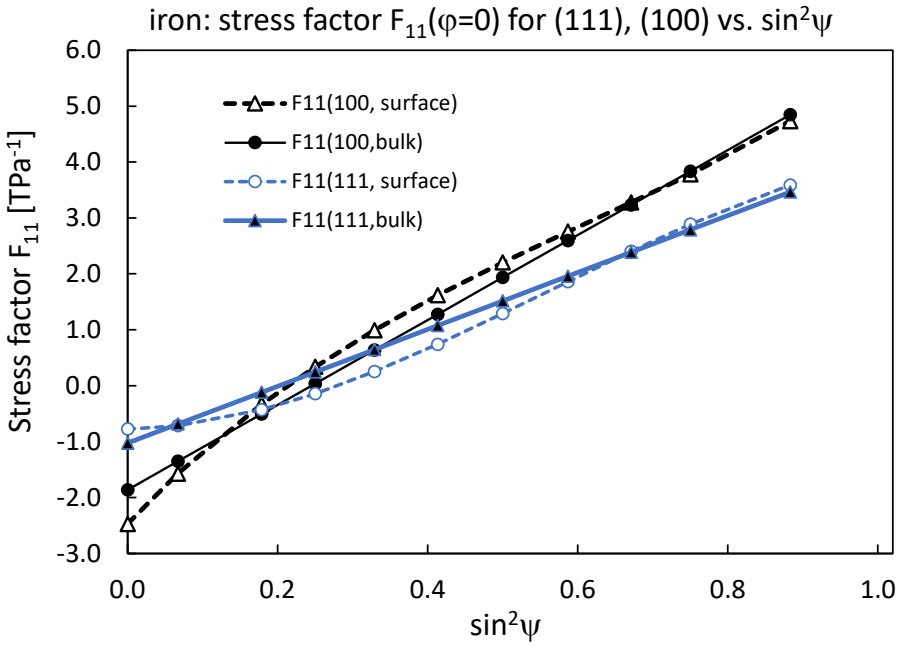

a)

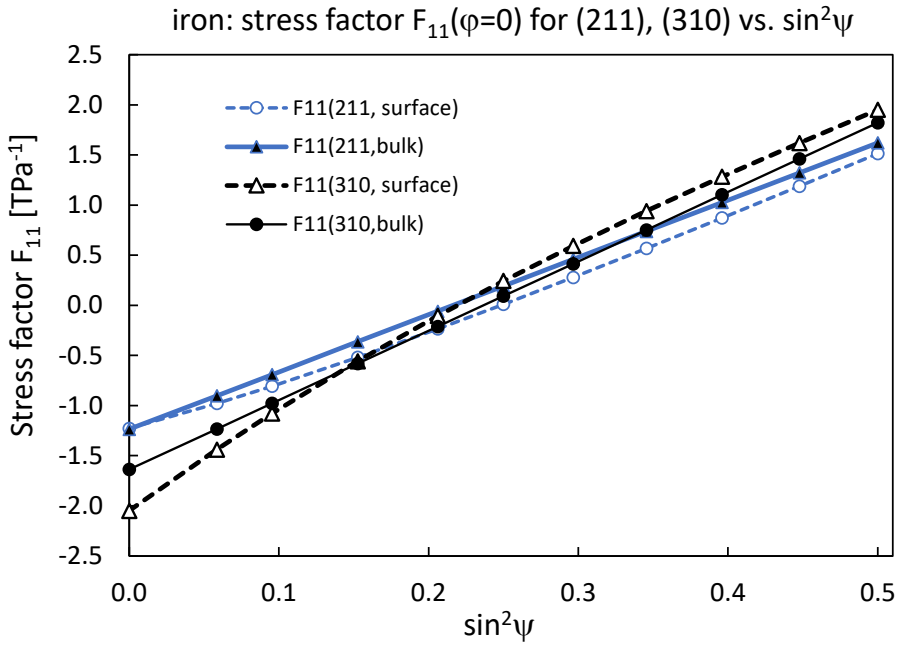

b)

Figure 3 Stress factor representation of XEC vs. tilt angle ψ (as $\sin^2\psi$) for iron. The graph of the left (a) shows the elastically softest (100) and the hardest (111) crystal directions. The right side graph (b) the (211) (using Cr-Kα) and (310) (using Co-Kα) are shown for a tilt range of 45°.

The (310) is the other iron reflection commonly used for stress measurements, and the surface effect is more pronounced with ≈25 % relative difference (F_{11}(310, ψ=0, surface) = -2.05 TPa^{-1} vs. F_{11}(310, ψ=0, bulk) = -1.64 TPa^{-1}) directly at the surface in the normal direction. Actual measurements may only partially reflect the surface effect due to the depth averaging in equation (12). Also, the surface XEC quickly converge with bulk XEC as the tilt angle increases.

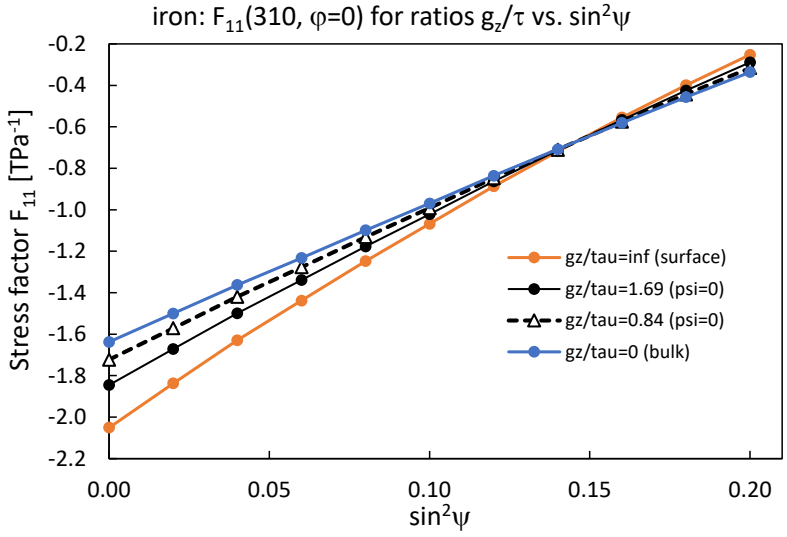

Figure 4 Stress factor F_{11}(310,0,ψ) calculated for Co-Kα with 1/μ=24 micron (see equation (11) for calculating τ) and grain sizes of 10 micron ($\frac{g_z}{\tau} = 0.84$) and 20 micron ($\frac{g_z}{\tau}$ =1.69) respectively. The $\sin^2\psi$ range shown is equivalent to a range of 25° in ψ.

For a strong surface effect ($\tau << g_z$) the isotropic approximation of using the ψ-independent $\frac{1}{2}s_2(hkl)$ and $s_1(hkl)$ may lead to systematic overestimation of stresses for 3Γ(hkl) < 0.75 (see Figure 4, g_z/τ=0); underestimation of stresses would occur for 3Γ(hkl) > 0.75 of the stress state. The opposite situation occurs for materials such as niobium where the elastic anisotropy is reversed (directional Young's modulus E(100) > E(111)). A numerical analysis of the effect is shown for the common iron reflections (211) and (310) in Figure 3b and Figure 4.

Table 1:Stresses evaluated using bulk XEC from strains that were simulated for the surface effect (surface XEC) on iron at 100 MPa stress. Results were obtained for different ranges of the tilt angle ψ and different ratios of z-thickness of the surface grain layer to the penetration depth τ. Each tilt angle range was subdivided into 10 intervals equidistant in $\sin^2\psi$ and strains were calculated for 100 MPa using the surface effect model after which the stress was determined, this time using bulk XEC. For the (310) the attenuation length for Co-Kα (λ=0.178892 nm) is 24 μm while for the (211) the attenuation length is 12 μm (using Cr- Kα with λ=2.28962 nm). Attenuation lengths were taken from [20].

(hkl)	g_z/τ	Grain size	ψ_{max} =26.8° Stress [MPa]	ψ_{max} =45° Stress [MPa]	ψ_{max} =60° Stress [MPa]
(310)	Inf.	-	136.8	114.8	104.6
(310)	1.69	20	118.9	108.4	102.3
(310)	0.84	10	107.9	103.8	101
(211)	Inf.	-	84.3	97.0	102.2
(211)	3.41	20	85.9	96.9	101.8
(211)	1.70	10	91.2	97.6	101.0

The results in Table 1, Figure 3, and Figure 4 suggest several ways of dealing with the surface effect in stress evaluation. First, if grain size information is available, the surface effect can be calculated for accurate estimation of stress. Second, the surface effect can be effectively minimized for stress analysis by reducing the contribution of strains measured at low tilt angles. This can be done either by choosing a sufficiently large tilt range with $\psi_{max} \geq 60°$ or under-sampling the strains in the surface sensitive tilt range $\leq 25°$, both of which reduce the overall contribution of surface sensitive strains to stress evaluation.

CONCLUSION

A model is developed for calculating the surface effect on X-ray elastic constants (XEC). The model is based on the assumption that surface grains can freely Poisson expand/contract in the normal direction as a response to in-plane stresses while maintaining the same grain-matrix interaction as bulk grains in-plane. X-ray penetration results in an absorption-weighted average of XEC at the surface and in the bulk, with the ratio of grain size to penetration depth as the governing factor. The surface effect is more pronounced both for lattice strain measurements in and near the surface normal direction and for higher degrees of elastic anisotropy. The latter implies that (hkl) with lattice plane normal vectors along elastically soft or hard directions are most sensitive to the surface effect. While the effect is generally small, X-ray stress measurements based on a single (hkl) can be systematically shifted to higher or lower values, depending on the (hkl).

REFERENCES

[1] R. D. Mindlin and D. H. Cheng, "Thermoelastic Stress in the Semi-Infinite Solid," *J. Appl. Phys.*, vol. 21, no. 9, pp. 931–933, Sep. 1950.

[2] K. Seo and T. Mura, "The Elastic Field in a Half Space Due to Ellipsoidal Inclusions With Uniform Dilatational Eigenstrains," *J. Appl. Mech.*, vol. 46, no. 3, pp. 568–572, Sep. 1979.

[3] T. Mura, *Micromechanics of defects in solids*, vol. 3. Dordrecht: Springer Netherlands, 1987.

[4] J. D. Eshelby, "The determination of the elastic field of an ellipsoidal inclusion, and related problems," *Proc. R. Soc. London. Ser. A. Math. Phys. Sci.*, vol. 241, no. 1226, pp. 376–396, Aug. 1957.

[5] U. Welzel, M. Leoni, and E. J. Mittemeijer, "The determination of stresses in thin films; modelling elastic grain interaction," *Philos. Mag.*, vol. 83, no. 5, pp. 603–630, Jan. 2003.

[6] R. W. Vook and F. Witt, "Thermally Induced Strains in Evaporated Films," *J. Appl. Phys.*, vol. 36, no. 7, pp. 2169–2171, Jul. 1965.

[7] H. Möller and G. Martin, "Elastische Anisotropie und röntgenographische Spannungsmessung," *Mitteilungen des Kaiser-Wilhelm-Instituts für Eisenforsch.*, vol. 21, pp. 261–269, 1939.

[8] W. Voigt, *Lehrbuch der Kristallphysik*. Stuttgart, Germany: Teubner Verlag, 1928.

[9] C. Mareau, "The dependence of X-ray elastic constants with respect to the penetration depth," *J. Appl. Crystallogr.*, vol. 56, no. 5, pp. 1446–1455, Oct. 2023.

[10] H. Behnken and V. Hauck, "Berechnung der roentgenographischen Elastizitaetskonstanten (REK) des Vielkristalls aus den Einkristalldaten fuer beliebige Kristallsymmetrie," *Zeitschrift für Met.*, vol. 77, no. 9, pp. 620–626, 1986.

[11] T. Gnäupel-Herold, A. A. Creuziger, and M. Iadicola, "A model for calculating diffraction elastic constants," *J. Appl. Crystallogr.*, vol. 45, no. 2, pp. 197–206, 2012.

[12] E. Kröner, "Berechnung der elastischen Konstanten des Vielkristalls aus den Konstanten des Einkristalls," *Zeitschrift für Phys. A*, vol. 151, no. 4, pp. 504–518, 1958.

[13] L. J. Walpole, “On the overall elastic moduli of composite materials,” *J. Mech. Phys. Solids*, vol. 17, no. 4, pp. 235–251, Sep. 1969.

[14] P. R. Morris, “Elastic constants of polycrystals,” *Int. J. Eng. Sci.*, vol. 8, no. 1, pp. 49–61, Jan. 1970.

[15] E. H. Bollenrath, F., Hauk, V., Müller, “On the calculation of polycrystalline elasticity constants from single crystal data,” *Zeitschrift für Met.*, vol. 58, pp. 76–82, 1967.

[16] T. Gnäupel-Herold, “Elastic behaviour of orientation-correlated grains in multiphase aggregates,” *J. Appl. Crystallogr.*, vol. 56, pp. 1658–1673, 2023.

[17] C. Genzel, “Formalism for the evaluation of strongly non-linear surface stress fields by X-ray diffraction performed in the scattering vector mode,” *Phys. Status Solidi*, vol. 146, no. 2, pp. 629–637, Dec. 1994.

[18] J. J. Adams, D. S. Agosta, R. G. Leisure, and H. Ledbetter, “Elastic constants of monocrystal iron from 3to500K,” *J. Appl. Phys.*, vol. 100, no. 11, Dec. 2006.

[19] R. F. S. Hearmon, “The elastic constants of anisotropic materials—II,” *Adv. Phys.*, vol. 5, no. 19, pp. 323–382, Jul. 1956.

[20] B. L. Henke, E. M. Gullikson, and J. C. Davis, “X-Ray Interactions: Photoabsorption, Scattering, Transmission, and Reflection at E = 50-30,000 eV, Z = 1-92,” *At. Data Nucl. Data Tables*, vol. 54, no. 2, pp. 181–342, Jul. 1993.